Available online at www.sciencedirect.com
ScienceDirect
Journal of the European Ceramic Society 26 (2006) 3307–3313
www.elsevier.com/locate/jeurceramsoc

Comparison between barium and strontium-glass composites for sealing SOFCs

M. Brochu, B.D. Gauntt, R. Shah, G. Miyake, R.E. Loehman *

Sandia National Laboratories, Advanced Materials Laboratory, 1001 University SE, Albuquerque, NM 87106, USA

Received 5 March 2005; received in revised form 29 July 2005; accepted 4 August 2005
Available online 5 October 2005

Abstract

The present study demonstrates the feasibility of adding micron-scale Y_2O_3-stabilized ZrO_2 (YSZ) powders to modify the properties of two borate glasses used for sealing electrolyte supported SOFCs. The crystallization of the composite made with a Ba-containing glass was found to be independent of the volume fraction of YSZ, as opposed to the situation for Sr-glass composites where the crystallization temperature decreased with the volume fraction of YSZ. The variation of the flow properties of both glass composites was measured using a wettability test, and an increase of the contact angle was measured when the volume fraction of additives was increased. Examining the microstructure showed that initially the Ba-containing glass reacted with YSZ to form a $BaZrO_3$ compound. Long time exposure at 800 °C caused a large reduction of the coefficient of thermal expansion (CTE), which is explained by increased formation of $BaZrO_3$ and further change in glass composition. On the other hand, the reaction involving the Sr-containing glass with the YSZ additive shows the initial formation of calcium zirconate (Ca is an ingredient in both glasses) followed by appearance of strontium zirconate with further heating. For this Sr glass composition, the observed reduction of CTE was associated with the change in composition of the remaining glassy phase since the CTEs of the reaction products are close to the CTE of the YSZ additives.

Keywords: Joining; Composites; Glass ceramics; ZrO_2; Fuel cells; Sealants

1. Introduction

A solid oxide fuel cell (SOFC) is an energy conversion device that generates electricity by electrochemically reacting a gaseous fuel (H_2, CH_4) on the anodic side with an oxidizing gas (O_2) coming from the cathode via ion-conduction through the electrolyte. The chief characteristic of a fuel cell is its ability to convert chemical energy directly into electrical energy without the need for combustion, giving higher conversion efficiencies than steam turbines or internal combustion engines, and resulting in more environmentally friendly power sources.[1–3]

The development of reliable sealing techniques is crucial for the commercialization of SOFCs. The power output of a single cell can be multiplied if a series of cells are connected through gas tight seals, which illustrates the importance of developing reliable joining methods for such systems. Among the numerous available joining techniques, using glass seals for SOFCs is the most attractive, in our opinion, due to the inertness to oxidizing and reducing atmospheres and self healing properties at service temperature higher than T_g. Implementing glass seals for SOFCs requires control of seal properties such as viscosity, flow, adhesion, thermal expansion, and reactivity, all of which are key limitations for the manufacture of SOFCs stacks.

A variant of conventional glass sealing uses well-defined heat treatment to nucleate and grow crystalline phases in the glass, which stabilizes the high temperature properties of the resulting composite. However, the control of the seal properties using this approach is restricted by the formation of thermodynamically favorable compounds only, limiting the operating window for engineering particular seal properties. Our novel approach allows the properties of the glass and ceramic phases of the composite to be optimized independently by the addition of unreactive particles to a glass matrix. Therefore, properties such as viscosity and CTE for example, are tailorable following theories used to predict the behavior of composite materials.

* Corresponding author. Tel.: +1 505 272 7601; fax: +1 505 272 7304.
E-mail address: loehman@sandia.gov (R.E. Loehman).

0955-2219/$ – see front matter © 2005 Elsevier Ltd. All rights reserved.
doi:10.1016/j.jeurceramsoc.2005.08.002

Prior research showed that all the glasses studied here wet and adhere to YSZ electrolyte structures.[4] Thus, bonding and sealing to SOFC electrolytes was not an issue in the present research. The objective of this work was to demonstrate the advantages of using glass composites over conventional glass seals for tailoring SOFC seal properties such as CTE, viscosity and reactivity. This novel approach was applied to an electrolyte-supported cell design.

2. Experimental procedures

Two borate glasses were used in this study because it is known that silicon diffusion from silicate glasses poisons the SOFC electrolyte by decreasing its ionic conductivity.[5] The borate glasses contain 40% B_2O_3, 10% Al_2O_3, 20% MgO, 20% CaO and 10% BaO–SrO for the Ba and Sr-compositions, respectively. The glasses were synthesized by calcining and melting their respective carbonates and oxides in a platinum crucible at 1500 °C for 2 h, then casting and annealing at 615 °C for 4 h. The cast ingots were ground in a vibratory mill to obtain a particle size distribution of −270 mesh. A high-purity YSZ powder (TZ-3Y, Tosoh) was used as the additive. The composite mixtures were produced by mixing and blending the respective ratio of glass and additive in a mill for 10 min. The composite mixtures were cold pressed either into (1) disks of 6.35 mm in diameter by 3 mm in thickness for thermal analysis, wettability and microstructure measurements or (2) bars of 50 mm × 6.35 mm × 3 mm for the measurement of the coefficient of thermal expansion. In each case, the green bodies were sintered at 50 °C above their respective T_gs to provide some mechanical strength for further handling.

The measurement of the thermal events that might occur during sealing was performed using Differential Thermal Analysis (DTA) in a TA Instruments STD-2960 machine using platinum crucibles. The samples were heated at 10 °C/min from room temperature to 1000 °C. Flowing dry air (0.125 L/min) was maintained during the cycle.

The wetting experiments were carried out in a Thermolyne 21100 tubular air furnace using an alumina muffle tube. The composite disks were centered on YSZ substrates (1 cm × 1 cm × 100 μm) and inserted into the furnace at room temperature and then heated at 20 °C/min up to the test temperatures (900 and 950 °C). The samples were soaked for 10 min and photographs of wetting profiles were acquired at 1 min intervals.

Cross sections of selected samples were mounted and automatically polished down to 0.25 μm using an automatic polishing machine (Buehler Ecomet 3®). The final polishing (0.05 μm colloidal silica) was performed on a Vibromet 2® for 2 h. The microstructures were examined with a JEOL-5800LV scanning electron microscope coupled with an Oxford EDS system. The samples were carbon coated prior to examination. The phase analysis was carried out on powder samples in a Siemens D500 diffractometer (Cu Kα radiation) between 20° and 70° at 0.05°/step for 1 s dwell time.

The CTE was measured between 50 and 550 °C using a Netzsch 402 ED dual rod dilatometer. A 25 mm sapphire standard was used and the measurements were performed in stagnant air. The samples were then aged in a box furnace in air at 800 °C for 50 and 200 h and the variation of CTE was measured after each holding time.

3. Results and discussion

3.1. Crystallization behavior of glass composites

Table 1 presents DTA measurements of the alteration of the characteristic thermal events of both glasses by the presence of YSZ additives during heating typical of a sealing cycle.

For the Ba-containing glass, the presence of YSZ powder decreases slightly the glass transition temperature and increases slightly the onset of crystallization and crystallization peak temperatures. The species that crystallize are discussed in Sections 3.3.1 and 3.3.2. By analogy with other glass systems, the alteration of the thermal events can be related to the level of solubility of ZrO_2 in this B_2O_3-glass. In a silicate glass system, Sawai[6] reported that the slight solubility of ZrO_2 is responsible for a reduction of the viscosity. A similar phenomenon could occur in this glass-composite system, explaining the reduction of the T_g. In a borosilicate glass, the solubility of ZrO_2 was associated with a structural change in the boron network, retarding phase separation.[7] Similarly, the dissolution of ZrO_2 in our Ba-glass may suppress the nucleation and growth of crystalline phases, explaining the higher temperature for onset of crystallization and crystallization peak observed. The volume fraction of YSZ additive seems to have no influence on these thermal events because the ZrO_2 solubility in the melt is so low that it is saturated even for the lowest amount used. Thus, we can vary the volume fraction of additive over a wide range for control of other properties such as flow and thermal expansion in the Ba-glass/YSZ system.

On the other hand, the Sr-containing glass behaves like a more conventional glass-ceramic. The YSZ additive has no influence on the T_g and a reduction of the onset of crystallization and crystallization peak temperature with YSZ volume fraction is observed. The invariance in T_g for the Sr glass system suggests the base glass is unchanged by the crystallization. In this case, the additive may act primarily as a conventional nucleating agent, facilitating the devitrification of the glass system. This possibility is supported by the gradual reduction of the onset of crystallization and crystallization peak temperatures with the volume fraction as a higher number of nucleation sites is present for the YSZ-Sr glass composites.

Table 1
Thermal events for Ba- and Sr-glass composites

Composite mixture	T_g (°C)	Onset crystallize (°C)	Crystallization peak (°C)
Ba-glass	584.7	749.3	785.2
Ba-glass + 5% YSZ	580.9	756.2	793.5
Ba-glass + 20% YSZ	581.3	760.3	799.1
Sr-glass	588.9	763.5	794.1
Sr-glass + 5% YSZ	589.2	754.2	784.0
Sr-glass + 20% YSZ	588.2	744.6	766.9

3.2. Wettability and flow properties

The wetting and spreading curves for both glass-composite compositions measured on YSZ plates at 900 and 950 °C for mixtures varying between 0 and 30 vol.% YSZ powder are presented in Fig. 1.

The spreading curves measured for the Ba-containing glass at 900 °C show a slight difference in final contact angle between the pure glass and the composite containing 2.5 vol.% (15° versus 22°). Similar increase in contact angle was observed for the 5 vol.% YSZ composite (37°). For mixtures with 10% YSZ and above, the disk retained its original shape, i.e. a contact angle of 90°. The measurements performed at 950 °C show the expected decrease in glass viscosity with this 50 °C rise in temperature. A reduction of the contact angle is observed for all mixtures below 20 vol.% YSZ. Similar difference in the contact angle is observed between the pure glass and the mixture containing 2.5 vol.% YSZ (1° versus 12°). The contact angle of the composite containing 5 vol.% YSZ decreases from 37° to 24° as the temperature increases from 900 to 950 °C, while the 10 vol.% YSZ possesses a 70° angle at 950 °C.

The wetting curves for the Sr-glass composites show that under comparable conditions, this system is more fluid than the Ba-glass composite system. At 900 °C, the pure Sr-based glass exhibits complete wetting on YSZ. The addition of 2.5 or 5% YSZ powder causes an increase of the contact angle when compared to the pure glass (10°–12° versus 1°) but no significant difference in θ was observed between these two YSZ volume fractions. Doubling the volume fraction to 10% YSZ increases the contact angle at 900 °C to nearly 40°. A major change in the composite viscosity was observed for 20 vol.% YSZ and above, where no flow was observed at 900 °C. The composite disks retained their original shape throughout the complete cycle. As opposed to the measurement taken at 900 °C, the equilibrium contact angle was already reached at the beginning of the test at 950 °C and no decrease in θ with time was observed. No difference in contact angle at 950 °C was observed between the pure glass and the composites containing 2.5 or 5 vol.%, YSZ. The addition of 10 vol.% YSZ raises the contact angle to 13° at 950 °C. Similar to the 900 °C results, the mixtures containing 20 and 30 vol.% YSZ powder show a major increase in composite viscosity, where contact angles of 78° and 90° (unchanged drop shape) were measured.

These results confirm that the viscosity of a glass-composite seal can be engineered by the addition of unreactive particles. In an unreactive composite system, the viscosity is controlled mainly by two factors: (1) the particle size and aspect ratio and (2) the volume fraction.[8] In our case, the same additive was used, removing the particle shape and size variable. Therefore, the higher volume fraction of YSZ causes the increase in viscosity of the glass composite. By comparing the two glass systems, our results show that, independent of the testing temperature, the Ba-containing composites exhibit a more viscous behavior compared to the Sr-containing composites, suggesting that the Ba-containing glass possesses a higher intrinsic viscosity. An additive level of only 10% is required to retard the spreading of the Ba-glass composite for a sealing cycle performed at 900 °C. A higher volume fraction of added powder counteracts the decrease in glass viscosity with temperature and allow sealing at higher temperature. On the other hand, at least 20 vol.% YSZ is needed to ensure proper reten-

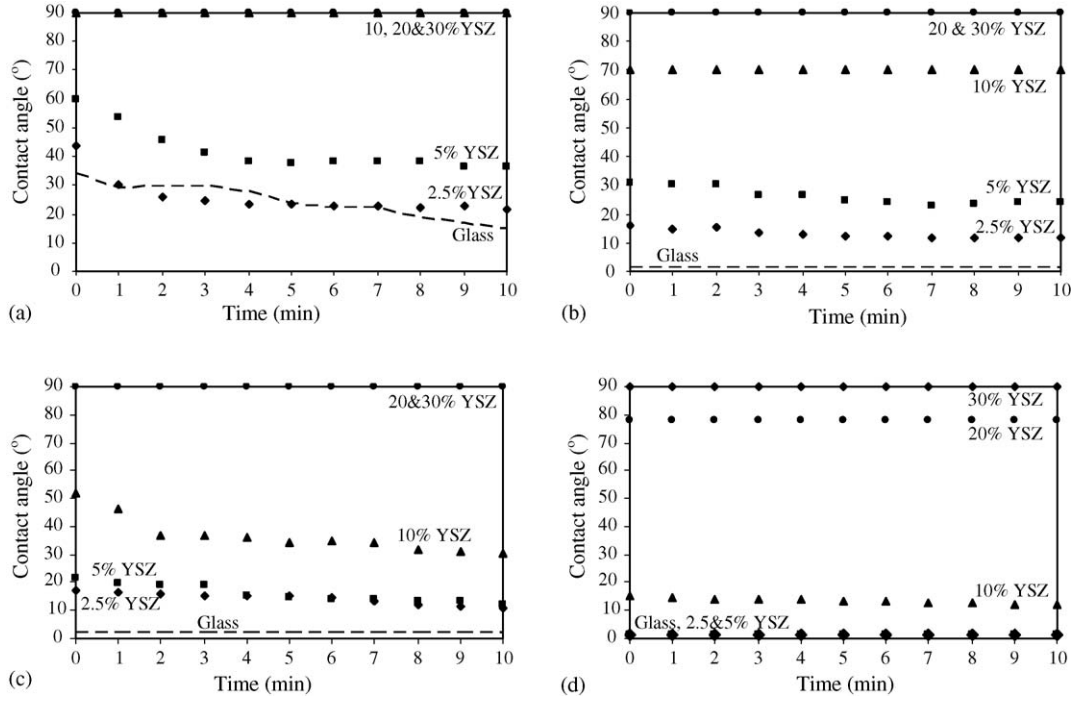

Fig. 1. Contact angle measurements on YSZ substrates for Ba-glass composites at (a) 900 °C and (b) 950 °C and for Sr-glass composites at (c) 900 °C and (d) 950 °C.

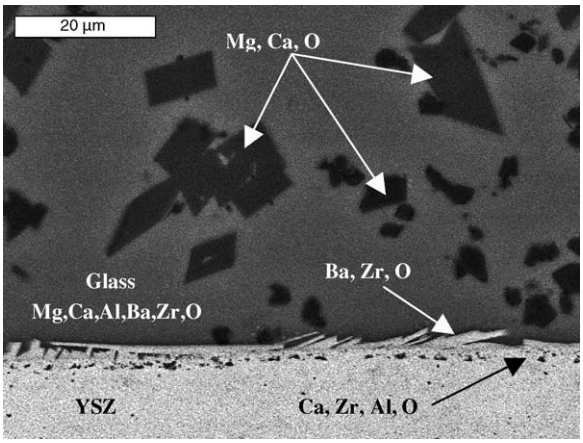

Fig. 2. Backscattered micrograph of interface between Ba-glass and YSZ after a sealing cycle of 10 min at 900 °C.

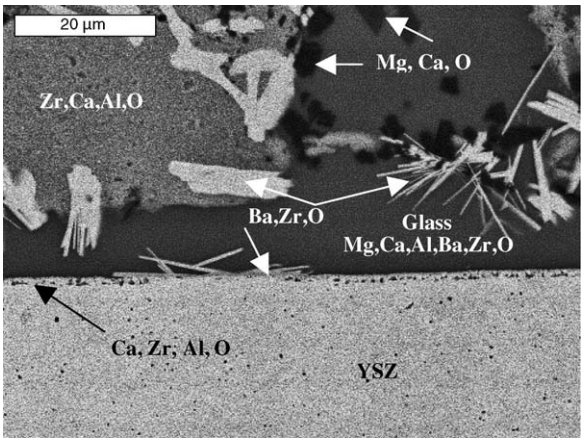

Fig. 3. Backscattered micrograph of interface between Ba-glass 20%YSZ composite and YSZ after a sealing cycle of 10 min at 950 °C.

tion of the seal geometry at 900 °C for the Sr-glass. Similarly to the Ba-containing composites, a higher volume fraction of YSZ should be used for a sealing cycle performed at higher temperature.

3.3. Microstructure and phase analysis

3.3.1. Ba-glass composites with YSZ

Fig. 2 presents a back-scattered electron micrograph of a pure Ba-glass/YSZ interface after a sealing cycle of 10 min at 900 °C. Two crystalline phases (darker phase) are present in the residual glass. In both cases, the EDS analysis detected Mg, Ca and O in these precipitates, but with different relative intensities. No B was detected due to the limitation of the EDS detector. One crystalline phase was identified as $MgCaB_2O_5$ using XRD. However, the main feature observed is the formation of a layered interfacial reaction layer. The EDS analysis detected the presence of Zr, Ca, Al and O at the interface with the YSZ substrate, suggesting the formation of Ca-containing ZrO_2 (fluorite structure) and $CaZrO_3$. The EDS analysis also detected the presence of Zr, Ba and O, suggesting the formation of $BaZrO_3$. The presence of this zirconate was validated with XRD. Finally, EDS analysis on the glassy phase showed a small peak of Zr, suggesting a certain level of solubility of ZrO_2 in the glass.

Fig. 3 presents a back-scattered electron micrograph of the interface between YSZ and a Ba-glass composite containing 20 vol.% YSZ after a sealing cycle of 10 min at 950 °C. Similar to the microstructure observed in the pure glass after sealing, there is a $BaZrO_3$ phase near the YSZ substrate and a $MgCaB_2O_5$ crystalline phase further into the bulk. The thin reaction layer containing Zr, Ca, Al and O is also observed at the interface with the YSZ substrate. Compared to the pure glass-YSZ experiments, the glass reacts extensively with the YSZ additive since a $BaZrO_3$ phase is also observed at the surface of the YSZ additive. EDS analysis on a YSZ particle shows, in addition to Zr and O, the presence of Ca and Al, suggesting elemental diffusion from the bulk glass. The Ca and Al peaks were not detected in the bulk of the YSZ substrate. Finally, the EDS analysis suggested an increased concentration of Zr present in the remaining glassy phase.

The ZrO_2–BaO binary phase diagram shows that the ZrO_2-rich portion contains a two-phase region composed of ZrO_2 and $BaZrO_3$.[9] Consistent with the phase diagram, $BaZrO_3$ crystals are observed on the YSZ particle surfaces in these experiments. The EDS analysis of the original YSZ phase near the glass interface after the sealing cycle shows Al and Ca peaks. Calcium oxide is well known to stabilize ZrO_2 in the fluorite structure.[10] The ZrO_2–Al_2O_3 phase diagram shows the typical binary that contains an eutectic at 38 mol% ZrO_2 with limited mutual solubility.[11] Muromura and Hinatsu[12] studied the ternary ZrO_2–CaO–Al_2O_3 phase diagram and they found that up to 4 mol.% Al_2O_3 is soluble in the fluorite structure. As no ZrO_2–Y_2O_3–CaO phase diagram is available, we postulate that the change in microstructure of the original YSZ is controlled by CaO diffusion to form the fluorite structure in the partially stabilized YSZ while simultaneously allowing some solubility of Al_2O_3, which results in a barium zirconate phase that contains Al_2O_3 and CaO in solid solution. The ZrO_2–BaO–Al_2O_3 phase diagram[13] shows a small solubility of Al_2O_3 in $BaZrO_3$, which explains the detection of an Al peak with the EDS analysis. The detection of the Ca peak confirms partial solubility of CaO in ZrO_2.

$CaMgB_2O_5$ phase was identified using X-ray diffractometry. This phase is identified in Figs. 2 and 3 by the arrows showing Mg, Ca and O, collected from the EDS spectrum. The absence of Zr, Ba and Y in this crystalline phase supports the results obtained by DTA and confirms the independence of the crystallization behavior of the glass-system from the presence of the YSZ powder additive. In addition, the detection of Zr in the EDS analysis on the glass matrix supports our belief that the delay of crystallization observed in the DTA traces for the glass composite is due to the change in the borate glass network from partial dissolution of ZrO_2 in the glass.

3.3.2. Sr-glass composites with YSZ

Fig. 4 presents a back-scattered electron micrograph of a Sr-glass/YSZ interface after a sealing cycle of 10 min at 900 °C. As opposed to the Ba-glass, no reaction product is observed but instead, the surface microstructure of the substrate has

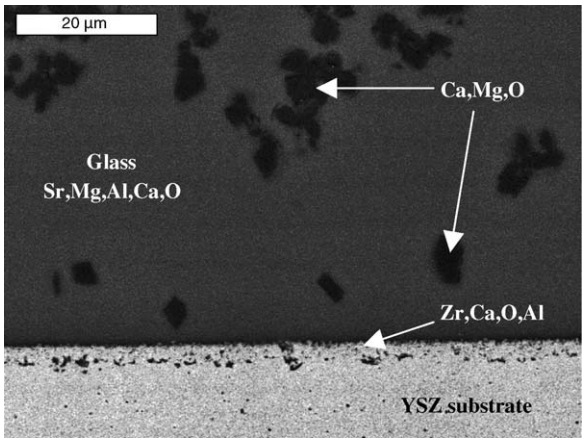

Fig. 4. Backscattered micrograph of interface between Sr-glass and YSZ after a sealing cycle of 10 min at 900 °C.

been altered. The EDS analysis of this layer shows the presence of Zr, Ca, O and traces of Al. The elemental analysis of the crystals indicates that the crystalline phase formed in this glass composition is similar to the crystals observed in the Ba-containing glass. The microstructure appears as if the molten glass has penetrated the YSZ grain boundaries very extensively. However, EDS analysis of the intergranular region does not show Sr, so any diffusion was not of the bulk glass composition. Finally, as opposed to the Ba-glass, no well defined Zr peak was detected on the glass phase near the YSZ substrate, suggesting lower solubility of ZrO_2 in this glass composition.

Fig. 5 presents a back-scattered electron micrograph of the interface between YSZ and the Sr-glass composite containing 20 vol.% YSZ after a sealing cycle of 10 min at 950 °C. Similar to the pure glass results above, the affected surface layer of the YSZ substrate is composed of Zr, Ca, O and traces of Al, and the crystalline phase away from the interface contains Mg, Ca and O. The surface of the YSZ powder additive contains two phases. The EDS analysis of the particle shows the presence of Zr, Ca, O, Al and Sr, suggesting that there is a different interaction between the glass and the YSZ particles than with the bulk YSZ substrate.

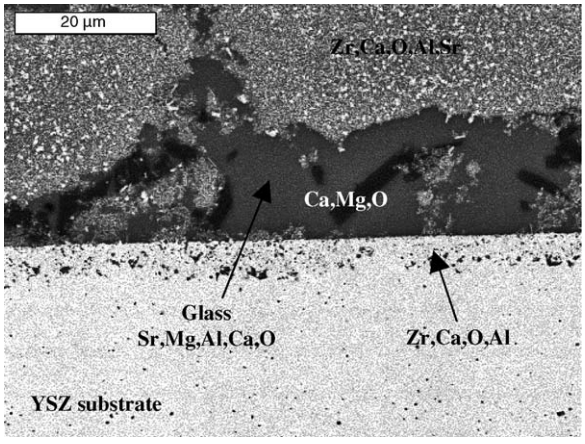

Fig. 5. Backscattered micrograph of interface between Ba-glass 20% YSZ composite and YSZ after a sealing cycle of 10 min at 950 °C.

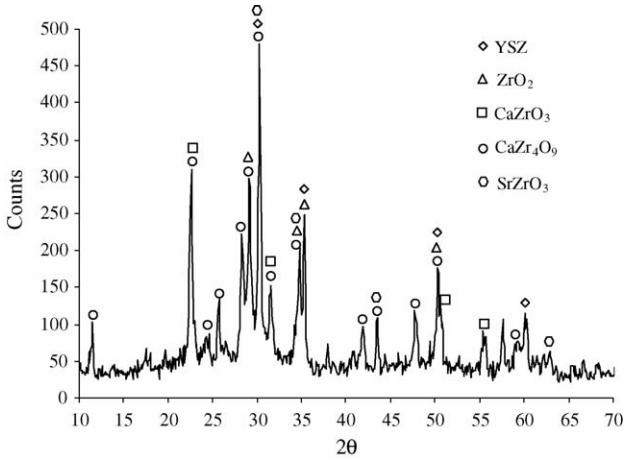

Fig. 6. XRD pattern of Sr-glass 20% YSZ composite after 50 h at 800 °C.

Finally, similarly to the case of pure glass, no distinct peak of Zr was detected in the residual glassy phase.

Fig. 6 presents the XRD pattern of a Sr-glass composite containing 20 vol.% YSZ after a sealing cycle at 900 °C for 20 min. The pattern exhibits a large number of peaks, which complicates the phase identification. Peaks of YSZ (JCPDS 30-1468) originating from the YSZ additive are detected. Other peaks can be associated with the monoclinic ZrO_2 (JCPDS 37-1484) phase. The majority of the remaining peaks can be attributed to the $CaZr_4O_9$ phase (JCPDS 28-0887), which according to the phase diagram is stable at high temperature and dissociates below 921 °C into a two-phase microstructure: a solid solution of monoclinic ZrO_2 and $CaZrO_3$. As observed, the main peaks of the ZrO_2 overlap with those from the $CaZr_4O_9$ phase. The reference spectrum for $CaZrO_3$ (JCPDS 35-0790) also shows that the major peaks of this compound overlap with those from $CaZr_4O_9$. Finally, $SrZrO_3$ peaks (JCPDS 23-0561) can also be identified in the pattern but they significantly overlap with peaks of YSZ or $CaZrO_4$.

The results obtained suggest that a two-step interaction involving CaO, SrO and ZrO_2 occurs during the sealing cycle. Based on the standard-state thermodynamics of formation of both crystalline compounds (Ca- and $SrZrO_3$) from their respective oxides, a lower ΔG_f^0 is calculated for $SrZrO_3$ and therefore it should be more stable than $CaZrO_3$.[14,15] However, the experimental detection of $CaZrO_3$ suggests that the sequence of the reaction products formed is also driven by kinetic factors, such as the initial quantity of CaO and SrO in the glass (chemical gradient) and the ionic rates of diffusion in the glassy phase. The Ca^{2+} should diffuse faster than Sr^{2+} because of its smaller ionic radius (1.00 versus 1.16 Å). According to the SEM/EDS observations and to the CaO–ZrO_2 phase diagram,[16] the bi-phase ZrO_2 and $CaZrO_3$ structure will form through initial diffusion from the glass and reaction of Ca^{2+} with the YSZ substrate, which is supported by the detection of Ca (no Sr) in the reaction layer between the pure glass and the YSZ substrate experiments.

The presence of YSZ additives in the glass composite will increase the consumption of the Ca^{2+} from the glass phase through the formation of $CaZrO_3$. The higher depletion of Ca^{2+} should then initiate the reaction between SrO and the residual

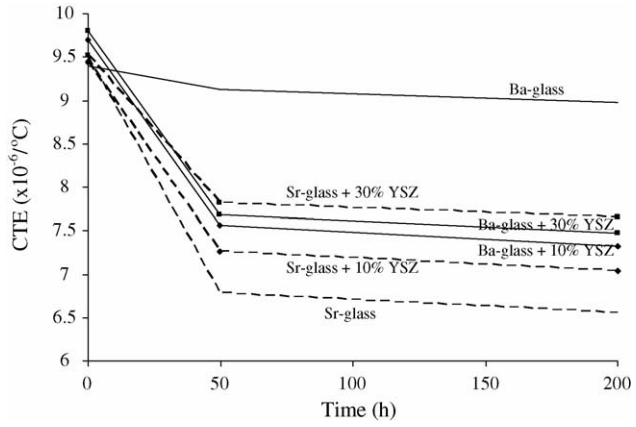

Fig. 7. Variation of the CTE for 0, 10 and 30 vol.% YSZ composite with Ba- and Sr-glass matrix for holding time at 800 °C.

YSZ to form $SrZrO_3$ given that the ZrO_2–SrO binary phase diagram shows no mutual solubility between the two compounds. This second SrO–YSZ reaction was not observed for the pure glass-YSZ substrate experiments because it is believed that the quantity of Ca^{2+} remaining in the glass phase was sufficient to sustain the preferential formation of $CaZrO_3$. However, in the composites, this second-step reaction between the glass and the YSZ additive is plausible as a Sr peak was detected by EDS. Note that our experiments could not distinguish between a ZrO_2–CaO–SrO solid solution and the formation of $SrZrO_3$ as most of the X-ray diffraction peaks of the $SrZrO_3$ overlap with other compounds present in the mixture and that no ZrO_2–CaO–SrO phase diagram is available.

3.4. Long term variation of glass and composite thermal expansion at service temperature

Fig. 7 presents the variation of the CTE of 10 and 30 vol.% composites as well as both pure glasses after holding times of 50 and 200 h at 800 °C. In all cases, the major change in CTE occurs within the first 50 h and only a slight reduction is observed during the next 150 h. In the case of the Ba-glass composites, after the sealing cycle (0 h) the CTE ranges between 9.4 and 9.7×10^{-6}/°C, where the CTE scales with the volume fraction of YSZ. After 50 h, the CTE of the pure glass decreases to 9.1×10^{-6}/°C, while a greater reduction is observed for the composites (7.57 and 7.68×10^{-6}/°C, for 10 and 30% YSZ, respectively). On the other hand, the Sr-glass and its composites possess CTEs that are identical within 0.1×10^{-6}/°C after the sealing cycle. The reduction of CTE after 50 h is greater for the pure Sr-glass (6.78×10^{-6}/°C) than for the 10 and 30% composites (7.26 and 7.82×10^{-6}/°C, respectively).

The variation of the CTE for composite materials can be predicted using Eq. (1):

$$\alpha_c = \alpha_g + (\alpha_a - \alpha_g)V_a \quad (1)$$

where α_c, α_g and α_a are respectively the coefficients of thermal expansion of the composite, the glass matrix and the additive and V_a is the volume fraction of additive. This equation predicts that in an unreactive system, the CTE of a composite varies with the volume fraction of additive. The Ba-glass composites follow the predictions of this equation after the sealing cycle as the CTE increases with the YSZ content. The slight reduction in the CTE for the pure glass after heating for 50 and 200 h at 800 °C is associated with the partial crystallization of the glassy phase through formation of $MgCaB_2O_5$. However, the greater reduction of the CTE of the two Ba-glass/YSZ composites after heating for 50 and 200 h at 800 °C is associated with partial crystallization of the glass and the formation of the $BaZrO_3$ phase from the reaction between the glass and the YSZ additive. Note that the CTE value of the calcium zirconate (10.4×10^{-6}/°C[17]) is close to the CTE of the YSZ and therefore has only a minor influence on CTE of the composite. Vassen et al.[17] reported that $BaZrO_3$ has a CTE of 7.9×10^{-6}/°C, which confirms that the presence of YSZ additive is responsible for greater reduction of CTE for the composite than for the pure glass because a higher volume fraction of $BaZrO_3$ is formed. The higher CTE value for the composite containing 30 vol.% YSZ compared to the 10 vol.% YSZ formulation is explained by the higher residual volume fraction of YSZ remaining in the composite once the BaO available in the glass as mostly reacted to form $BaZrO_3$ (CTE YSZ > CTE $BaZrO_3$).

The major reduction of CTE for the pure Sr-containing glass is associated with a lower value of CTE of the remaining glassy and crystalline phases upon devitrification after 50 and 200 h of holding time at 800 °C. The CTEs of the Sr-glass composites follow Eq. (1) after 50 and 200 h of holding time. The microstructure results confirmed reaction between the glass and the YSZ additive, which suggests that the CTE of the reaction products are near the CTE of YSZ. In fact, literature values reported for the CTE of both Ca and Sr-zirconates are close to the CTE of YSZ (10.9×10^{-6}/°C for $SrZrO_3$[17]). Therefore, the adjustment of the CTE of the glass-composite by the addition of YSZ additive is problematic for both glass-systems: formation of $BaZrO_3$ that possess low CTE for the Ba-containing glass system and low CTE for the pure Sr-glass after devitrification.

4. Conclusion

This study demonstrates that the properties of glass composite seals for sealing SOFCs can be tailored by the addition of YSZ powder to a borate glass for sealing electrolyte supported cells. For both glass composite studied, viscous flow is reduced in proportion to the volume fraction of added YSZ powder. Ba-containing glass shows extensive reaction with YSZ to form barium and calcium zirconate. The lower CTE of $BaZrO_3$ compared to the CTE of the glass is responsible for reducing the CTE of the composite. On the other hand, the interaction between the Sr-glass and the additive forms calcium and strontium zirconates, which have similar CTEs to the YSZ. The reduction of CTE observed for these composites after heating for 200 h at 800 °C is attributed to the change of composition of the remaining glassy phase after reaction and crystallization.

References

1. Minh, N., Ceramic fuel cells. *J. Am. Ceram. Soc.*, 1993, **76**(3), 563–588.

2. Yamamoto, O., Solid oxide fuel cells: fundamental aspects and prospects. *Electrochem. Acta*, 2000, **45**, 2423–2435.
3. Steale, B. C. H. and Heinzel, A., Materials for fuel cell technologies. *Nature*, 2001, **414**, 345–352.
4. Loehman, R. E., Dumm, H. P. and Hofer, H., Evaluation of sealing glasses for solid oxide fuel cells. *Ceram. Eng. Sci. Proc.*, 2002, **23**(3), 699–710.
5. Lee, J. H., Mori, T., Li, J. G., Ikegami, T., Komatsu, M. and Haneda, H., Improvement of grain-boundary conductivity of 8 mol.% yttria-stabilized zirconia by precursor scavenging of siliceous phase. *J. Electrochem. Soc.*, 2000, **147**(7), 2822–2829.
6. Sawai, I., *Glass Technol.*, 1961, **2**, 243.
7. Du, W. F., Kuroaka, K., Akai, T. and Yazawa, T., Effect of additive ZrO_2 on spinodal phase separation and pore distribution of borosilicate glasses. *J. Phys. Chem. B*, 2001, **105**(48), 11949–11954.
8. Ewsuk, K. G. and Harrison, L. W., Densification of glass-filled, alumina composites. In *Sintering of Advanced Ceramics in Ceramic Transactions*, *Vol. 7*, ed. C. A. Handwerker, J. E. Blendell and W. Kaysser. The American Ceramic Society, Westerville, OH, 1990, pp. 436–451.
9. Levin, E. M., Robbins, C. R. and McMurdie, H. F., *Phase Diagrams for Ceramists*, *Vol. 1*. The American Ceramic Society, 1981, p. 199.
10. Levin, E. M., Robbins, C. R. and McMurdie, H. F., *Phase Diagrams for Ceramists*, *Vol. 1*. The American Ceramic Society, 1981, p. 105.
11. Roth, R. S., Dennis, J. R. and McMurdie, H. F., *Phase Diagrams for Ceramists*, *Vol. 6*. The American Ceramic Society, 1987, p. 155.
12. Muromura, T. and Hinatsu, Y., Phase relation of ternary system ZrO_2–CaO–Al_2O_3. *Mater. Res. Bull.*, 1986, **21**, 61–67.
13. Roth, R. S., Negas, T. and Cook, L. P., *Phase Diagrams for Ceramists*, *Vol. 4*. The American Ceramic Society, 1981, p. 197.
14. Dash, S., Singh, Z., Prasad, R. and Sood, D. D., The standard molar Gibbs free energy of formation of $SrZrO_3$(cr). *J. Chem. Thermodyn.*, 1994, **26**, 307–314.
15. Brown, R. R. and Bennington, K. O., Thermodynamic properties of calcium zirconate ($CaZrO_3$). *Thermochim. Acta*, 1986, **106**, 183–190.
16. Du, Y., Jin, Z. and Huang, P., Thermodynamic calculation of the zirconia–calcia system. *J. Am. Ceram. Soc.*, 1992, **75**(11), 3040–3048.
17. Vassen, R., Cao, X., Tietz, F., Basu, D. and Stöver, D., Zirconates as new materials for thermal barrier coatings. *J. Am. Ceram. Soc.*, 2000, **83**(8), 2023–2028.